Submarine Paleoseismology Along Populated Transform Boundaries

The Enriquillo-Plantain-Garden Fault, Canal du Sud, Haiti, and the North Anatolian Fault, Marmara Sea, Turkey

BY CECILIA M.G. McHUGH, LEONARDO SEEBER, MARIE-HELENE CORMIER, AND MATTHEW HORNBACH

The Tapion Ridge structure related to a bend of the Enriquillo-Plantain-Garden fault. Based on coral reefs, Taylor et al. (2011) documented uplift events at 2,100-year recurrence intervals. The latest uplift was in 2010. The authors documented similar timing for the last two turbidites in Canal du Sud.

ABSTRACT. Continental transform boundaries cross heavily populated regions and are associated with destructive earthquakes worldwide. The devastating 1999 Turkey earthquakes and the offshore 2010 Haiti earthquake emphasized the urgent need to study the submerged segments of continental transforms. In response, the rapidly evolving field of submarine paleoseismology is focusing its attention on understanding the relationships between sedimentation, seafloor ruptures, and earthquake recurrence intervals along submarine faults. In Canal du Sud, Haiti, the 2010 earthquake-triggered sedimentation events were documented from nearshore to the deep basin by measuring the excess ^{234}Th in sediment cores. This radioisotope, with a half-life of 24 days, tracked mass wasting, turbidites, turbidite-homogenite units, and a sediment plume that remained in the water column for at least two months after the earthquake. However, the turbidite units in Canal du Sud, Haiti, provide an incomplete record of the region's earthquake history, likely because sedimentation rates are too low for sedimentation events to be triggered by all earthquakes. In contrast, in the Marmara Sea basins, there is very good correlation between turbidites and the historical record of earthquakes dating back 2,000 years. The difference between these correlations is likely related to both sedimentation rates and particulars of the ruptures. Future research along the Enriquillo-Plantain-Garden fault in Haiti and along similar low sedimentation plate boundaries should focus on multiple fault segments in order to obtain complete earthquake recurrence histories.

INTRODUCTION

The role of earthquake-induced sediment erosion, transport, and deposition at submerged continental transform boundaries is an important frontier in marine research. The destructive 2010 Haiti earthquake and the 1999 earthquakes in Turkey brought to the world's attention the need to investigate seafloor ruptures and earthquake recurrence intervals along submarine transform faults (e.g., Barka, 1999; Parsons et al., 2000; Reilinger et al., 2000; Calais et al., 2010; Hayes et al., 2010; Prentice et al., 2010). Many onshore-offshore continental transform boundaries exist near densely populated regions, and faulting at these transforms sometimes generates destructive earthquakes. Although transform faults have been extensively studied worldwide on land, these systems often

include submerged segments that are more difficult to study due to their locations and depths. Examples include the San Andreas fault system in the offshore California borderland (Plesch et al., 2007), the North Anatolian fault in the Marmara and Aegean Seas (Barka, 1999; Armijo et al., 1999), the Enriquillo-Plantain-Garden fault (EPGF) in Gonave Gulf, Haiti (Mann et al., 1995), and the El Pilar transform fault along the Venezuelan borderland (e.g., Schubert, 1982; Escalona et al., 2011). Shallow earthquakes that are small compared to great subduction earthquakes occur relatively frequently along these fault systems, but they can be disproportionally damaging as a result of both shaking and tsunami generation.

Here, we explore the relationship between earthquakes and sedimentation

along submerged continental transform boundaries. What role do earthquakes play in sediment erosion, transport, and deposition? Where are the best sedimentary records of earthquakes preserved? What techniques are best for identifying earthquake-generated deposits? In what circumstances can the sedimentary record yield long-term earthquake recurrence intervals? How do the relative rates of seismicity and sedimentation affect the correspondence between large earthquakes and sedimentation events? Addressing these questions is critical for geohazards assessment of heavily populated coastal regions such as Port-au-Prince, Haiti, and Istanbul, Turkey.

SUBMARINE PALEOSEISMOLOGY

The rapidly evolving field of submarine earthquake geology is advancing our understanding of sedimentation processes while simultaneously revealing new insights into prehistoric patterns of large earthquakes. The marine record has advantages over land records for obtaining a complete history of earthquakes because a much longer and continuous stratigraphy can be recovered and used for regional correlations. Most studies linking earthquakes to sedimentation events have focused on convergent plate boundaries, for example, the Cascadia subduction margin off western North America (e.g., Goldfinger et al., 2003, 2012; Gutiérrez-Pastor et al., 2013), offshore Galicia and Portugal (Gracia et al., 2010), the Chile Trench offshore Chile (St-Onge et al., 2012), the Hikurangi Trench offshore New Zealand (Pouderoux et al., 2012), the Calabrian

arc subduction system in the Ionian Sea (Polonia et al., 2012), the Kuril trough offshore Japan (Noda et al., 2008), the Sumatran subduction zone (Patton et al., 2013), and most recently the Japan Trench after the 2011 Tōhoku earthquake

> ## SUBMARINE PALEOSEISMOLOGY HAS SUCCESSFULLY EMERGED FROM THE INITIAL EXPERIMENTAL PHASE AND IS POISED TO BEAR MANY FRUITS.

(Strasser et al., 2013). The relationship between sedimentation events and earthquakes has also been investigated along transform plate boundaries, such as the North Anatolian fault beneath the Marmara Sea (Sari and Çağatay 2006; McHugh et al., 2006, 2014; Beck et al., 2007; Drab et al., 2012; Çağatay et al., 2012; Eris et al., 2012), the El Pilar fault in the Cariaco Basin, Venezuela (Thunell et al., 1999), the Alpine strike-slip fault in New Zealand (Barnes et al., 2013), and the EPGF offshore Haiti (Hornbach et al., 2010; McHugh et al., 2011a). Where available, long historical records allow correlation between sedimentation events and large earthquakes. For example, in Turkey, the historical earthquake record extends back 2,000 years (e.g., Ambraseys, 2002), but in Haiti it extends back only 500 years, making the linkage between sedimentation and earthquakes there more challenging and necessary (Bakum et al., 2012).

The evolving field of submarine paleoseismology also requires improvements of tools and techniques to characterize sedimentary deposits and distinguish those linked to seismic events from those that are not. High-resolution multibeam bathymetry provides the details of seafloor morphology (basins, channels, canyons, faults; e.g., Cormier et al., 2006). Subbottom profiling reveals the shallow subsurface strata that may be deformed, displaced, transported, or deposited during an earthquake (e.g., Beck et al., 2007; Brothers et al., 2009). Sediment coring in specific settings provides key information on the timing and distribution of sedimentation events. Geochemical and lithologic characteristics of the sediment can be measured at millimeter to centimeter scales (e.g., Çağatay et al., 2012; Drab et al., 2012; McHugh et al., 2014). Biostratigraphy analysis identifies the water depth from which the sediment failures originated (e.g., McHugh et al., 2011a). Based on these and other sediment analyses, mass wasting and gravity flows can be confidently identified and characterized.

Depocenters, the bathymetrically deepest and flattest parts of basins, are prime locations for recovering the most complete turbidite records. Submarine basins in tectonically active areas are often bounded on one side by a fault, and their floors tilt toward the fault, deepening with every earthquake rupture, thus providing space for new turbidite deposits (e.g., Seeber et al., 2006). Turbidity currents tend to reach the deepest part of a basin where they deposit most of the suspended sediment as their velocity and turbulence diminish. Thus, depocenters usually preserve the most complete stratigraphic record of turbidites. Lack of erosion and thick units are critical for unequivocal identification of the sedimentation event and establishment of reliable correlations between sites. Regional-scale correlations are essential for differentiating seismic from non-seismic events, and marine work is advantageous for identifying earthquake-generated deposits and characterizing fault segments.

Dating sedimentation events is challenging, but age models at a resolution necessary for correlating such events with earthquakes have been developed using short-lived isotopes and radiocarbon dating techniques, including Bayesian techniques such as OxCal for modeling radiocarbon ages (e.g., Çağatay et al., 2012; Drab et al., 2012; Goldfinger

Cecilia M.G. McHugh (cmchugh@qc.cuny.edu) is Professor, School of Earth and Environmental Sciences, Queens College, Flushing, NY, USA, and Senior Adjunct Researcher, Lamont-Doherty Earth Observatory of Columbia University, Palisades, NY, USA. Leonardo Seeber is Research Professor, Lamont-Doherty Earth Observatory of Columbia University, Palisades, NY, USA. Marie-Helene Cormier is Visiting Scientist, University of Rhode Island, Graduate School of Oceanography, Narragansett, RI, USA. Matthew Hornbach is Associate Professor, Southern Methodist University, Huffington Department of Earth Sciences, Dallas, TX, USA.

et al., 2012; McHugh et al., 2014). A sedimentation event such as a turbidite is identified and dated through chronostratigraphy and then correlated to the historical record of earthquakes, if available. This correlation needs to take into account uncertainties in both the sedimentation event chronology and the accuracy of the historical earthquake record. While dating is often the weakest constraint on the sediment side, location and magnitude are often the weakest constraints for historical earthquakes. These uncertainties are addressed through ground shaking studies, historical descriptions, and wave models.

THE 2010 HAITI EARTHQUAKE ALONG THE ENRIQUILLO-PLANTAIN-GARDEN FAULT

The motion between the Caribbean and North American Plates, along the northern boundary of the Caribbean Plate, is accommodated by two left-lateral and subparallel transform faults: the EPGF and the Septentrional fault (SF) (Mann et al., 1995; Dixon et al., 1998; Figure 1). GPS-derived surface motion is at a relative rate of 18–20 mm yr^{-1} (DeMets et al., 2000; Calais et al., 2010). Geodetical modeled rates are 12 ± 3 mm yr^{-1} for the SF and 6 ± 2 mm yr^{-1} for the EPGF. The EPGF crosses the southern peninsula in Haiti in an east-west direction (Figure 1). Modeling studies prior to the 2010 Haiti earthquake indicated that elastic strain had been accumulating along the EPGF and predicted that a fault rupture could occur (Manaker et al., 2008). The January 12, 2010, M7.0 earthquake occurred along or near the EPGF; it was an unusual tectonic event involving slip along multiple faults (e.g., Calais et al., 2010; Prentice et al., 2010; Hayes et al., 2010; Douilly et al.,
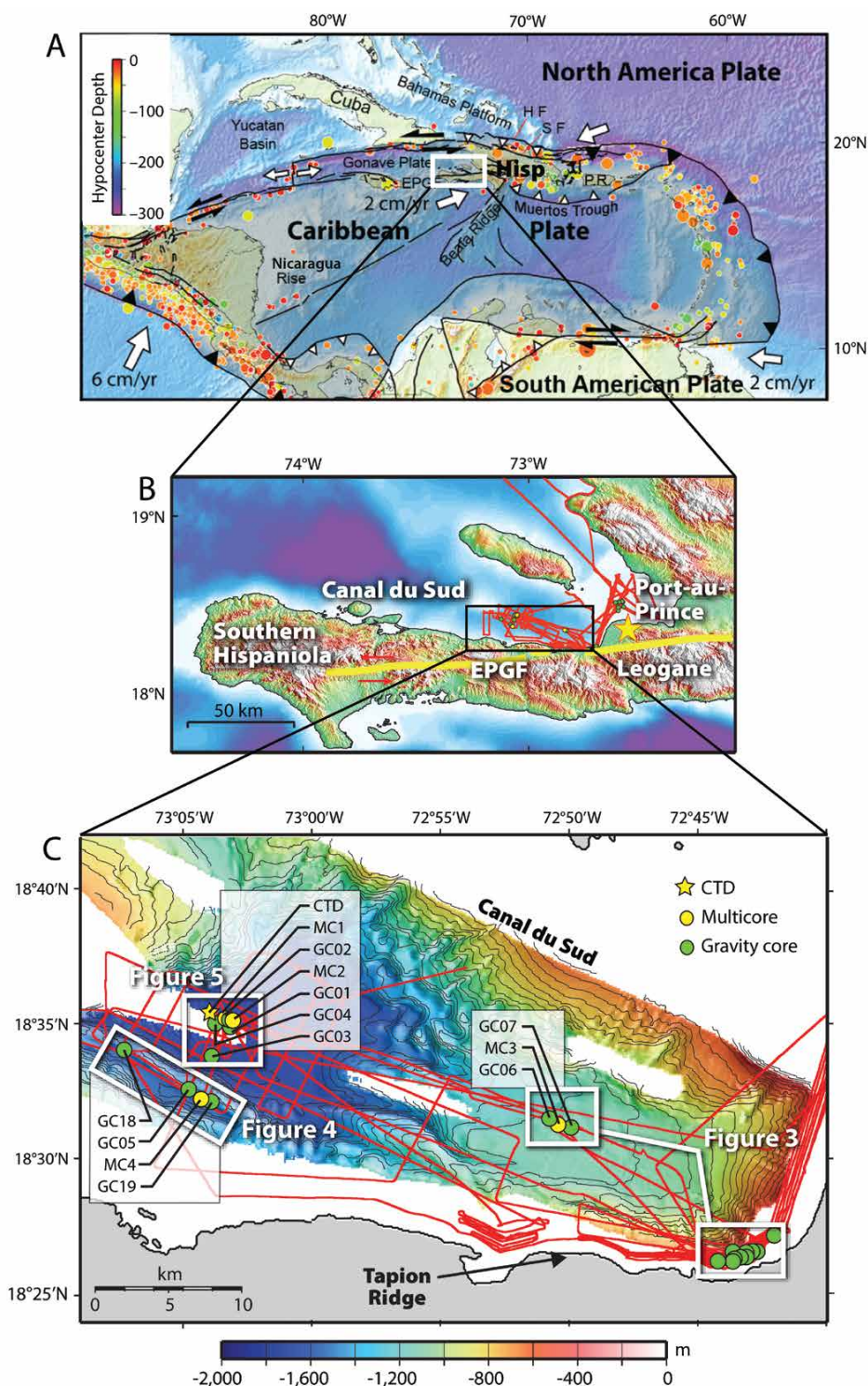

Figure 1. (A) Tectonic setting showing the relative motion between the Caribbean and North American Plates (white arrows). *Courtesy of E. Calais.* The study area (white box) is along the northern boundary of the Caribbean Plate where motion relative to the North American Plate is at an oblique angle and a left lateral transform boundary has developed. *Modified after McHugh et al. (2011a)* (B) The Enriquillo-Plantain-Garden fault (EPGF) is part of the plate boundary and crosses Southern Hispaniola (yellow line). The yellow star marks the epicenter of the 2010 Haiti earthquake. Cores, conductivity-temperature-depth (CTD) measurements, high-resolution subbottom profiles, and multibeam bathymetry were collected during an R/V *Endeavor* expedition (navigation tracks in red) in 2010 after the earthquake. (C) Multibeam bathymetry of Canal du Sud showing the location of the gravity cores (GCs; green circles), multicores (MCs; yellow circles), and CTD measurements (yellow star). The boxes locate Figures 3, 4, and 5. *Courtesy of Mercier de Lépinay*

2013). Although the main rupture was dominantly strike-slip, aftershocks yielded almost exclusively compressive (thrust) focal mechanisms, thus manifesting partitioning of the transpressive Caribbean-North American motion in a single sequence (Hough et al., 2010; Mercier de Lépinay et al., 2011; Douilly et al., 2013; Figure 1). The land portion of the rupture did not reach the surface (Prentice et al., 2010). GPS and satellite radar interferometric analysis confirmed that the earthquake was characterized by a significant reverse faulting component (at least 33–50%) in addition to left-lateral strike-slip (Calais et al., 2010; Hashimoto et al., 2011). The earthquake was catastrophic for Haiti, killing more than 50,000 people and devastating the capital Port-au-Prince and surrounding regions (Koehler et al., 2012). Deformation was documented along the submerged portions of the EPGF in Canal du Sud after the 2010 earthquake (Figure 2). CHIRP sub-bottom profiles reveal a series of folds (thrust fault anticlines) that are slightly oblique to the EPGF. The structural relief of the young folds increases from west to east toward the EPGF.

The 2010 earthquake triggered multiple nearshore sediment failures, generated turbidity currents, and stirred fine sediment into suspension throughout the basin (McHugh et al., 2011a). The earthquake also caused a tsunami that was directly related to deformation and indirectly to sediment failures (Hornbach et al., 2010). The sedimentation events generated by the earthquake were tracked with short-lived radioisotopes from the nearshore, across the slope, in fault basins, and in the deepest part of Canal du Sud basin, providing an exceptional opportunity to document and characterize earthquake-triggered sedimentation (McHugh et al., 2011a). The offshore segment of the EPGF across the shelf is manifested by two subparallel ridges that are ~ 100 m in relief (Figure 3A). Sediment cores were recovered adjacent to the ridges of the EPGF across the shelf in water depths of 150 m to 300 m. The cores show mixing of coarse sand, shells, and shell fragments in a muddy matrix (e.g., Figure 3B). The sediment also shows evidence of fluidization and brecciation and pervasive fracturing throughout the length of the cores (~ 150 cm). Cores GC08 through GC12 contained excess (xs) ^{234}Th activity (Table 1). The ^{234}Th radioisotope forms in the water column from the decay of uranium and is present in seafloor sediment; the additional ^{234}Th present
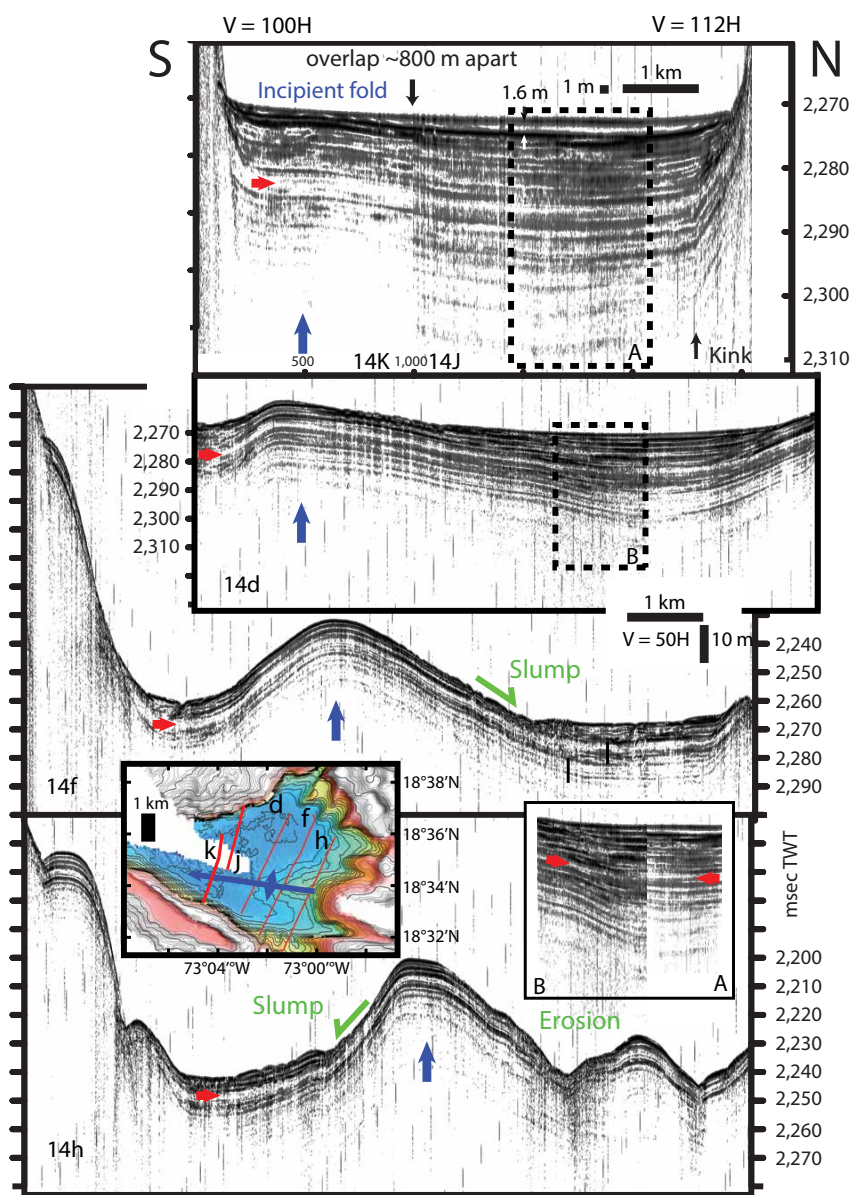

Figure 2. CHIRP subbottom profiles acquired from an R/V *Endeavor* expedition in 2010. The structural growth of the anticline (blue arrow) is shown from 1 m in the western profile (14K) to > 30 m in the easternmost profile (14h). The growth sequence indicates long-term growth of this young feature over many earthquake cycles.

in the core had been adsorbed rapidly to sediment that had been resuspended by the earthquake. Because xs^{234}Th has a half-life of 24 days, we could link the mass-wasting and turbidite deposits found in the core tops to the 2010 earthquake.

Thin, sand-rich turbidites with sharp basal contacts characterize slope sedimentation at 1,100 m water depth (Figure 3C,D). Generally, high-velocity turbidity currents cause more erosion than deposition along steeper slopes, eroding the substrate beneath and/or only preserving thin turbidites. The multicore MC3 that recovered the sediment-water interface, as well as gravity cores GC06 and GC07 recovered from the slope, contained xs^{234}Th on their tops, providing evidence of the 2010 event. In addition, the top turbidite contained abundant recent plant matter, confirming the link to the 2010 earthquake (McHugh et al, 2011a).

In a small fault-controlled basin (~ 5 km long; Figure 1) at 1,500 m water depth, the cores (GC05, 18, 19, and MC4) also contain high concentrations of xs^{234}Th (25.63 ± 68 dpm g^{-1}; dpm g^{-1} = decays per minute per gram of sediment) in the upper turbidite, linking the sediment to the 2010 earthquake (Figure 4).

The greatest sediment deposition occurred in the deepest part of the Canal du Sud at 1,730 m water depth. There, we recovered a ~ 60 cm thick turbidite blanketing the basin floor (GC01–GC04; MC1, MC2; Figure 5). The turbidite contains a 5 cm thick bed of cross-bedded sand with foraminifers of shallow water affinity and plant material (McHugh et al., 2011a). The sand is black and of volcanic origin rich in basaltic clasts and minerals derived from former oceanic basement rocks that are exposed in the southern Haitian peninsula (Vila et al., 1985). Rivers transport the sand into Canal du Sud deltas. Homogeneous mud, ~ 50 cm thick, and nearly barren
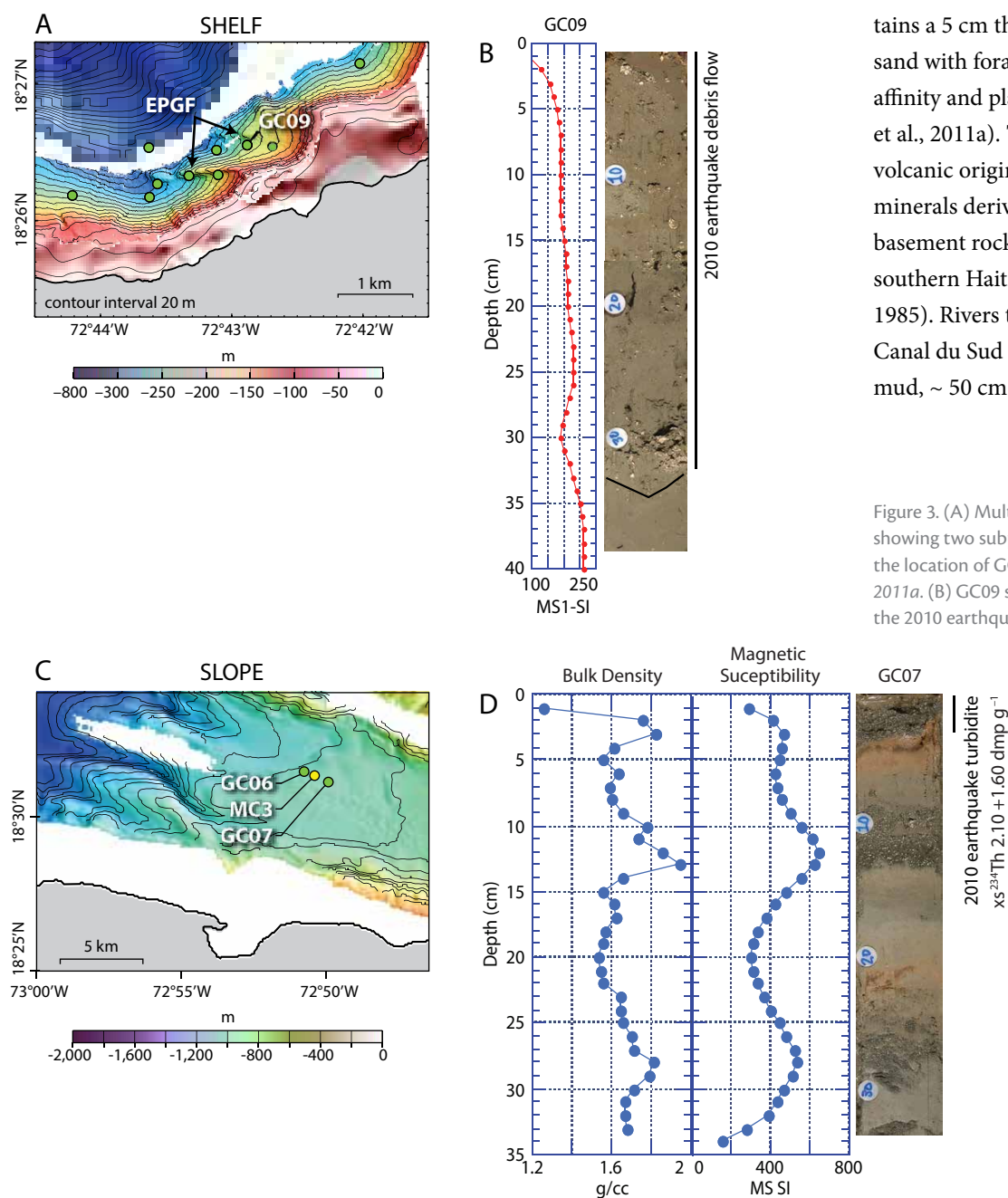

Figure 3. (A) Multibeam bathymetry of the shelf showing two subparallel ridges of the EPGF and the location of GCs. *Modified after McHugh et al., 2011a.* (B) GC09 shows mass wasting triggered by the 2010 earthquake as a chaotic mix of mud and shells. The magnetic susceptibility signal peaks at 25 cm due to the presence of sand and shells. (C) Multibeam bathymetry of the slope showing the location of GCs and MCs. (D) The 2010 earthquake turbidite is thin (5 cm) on cores recovered from the slope. In GC07, two other thin sandy turbidites are present beneath. The turbidites are separated by mud intervals interpreted as "normal" marine sedimentation. Sandy intervals are revealed by increases in bulk density and magnetic susceptibility. Excess ^{234}Th was measured in the top turbidite.

of microfossils was deposited above the sand layer. The sandy part of the turbidite and the muddy homogeneous deposit above it are together called a turbidite-homogenite unit (THU); they have identical geochemical elemental compositions, further evidence that both derived from a single earthquake-triggered event.

The 2010 THU was identified and dated in all cores recovered across the depocentral region (Figure 5, Table 2). A second, nearly identical THU was documented below it, and that older THU was dated at > 2,500 years BP. Surprisingly, the large historical 1770 and 1751 CE earthquakes (Bakum et al., 2012), as well as other earlier earthquakes that presumably shook the region, apparently did not trigger sedimentation events that reached the Canal du Sud depocenter at 1,730 m water depth. Interestingly, the same penultimate THU was dated at > 3,200 years BP in GC03 recovered along the Canal du Sud basin margin. Subbottom profiles reveal that this older sediment age is likely the result of erosion (of the upper 5 cm) along the margin of the basin. In the Marmara Sea, turbidites recovered from basin margins consistently have older ages. This is due to base-of-slope mass wasting processes and/or their location adjacent to a fault (McHugh et al., 2014). The Canal du Sud findings further confirm that basin depocenters preserve the best stratigraphic record of turbidites (Figure 5).

Lack of a complete sedimentary record of earthquakes in Canal du Sud is due, at least in part, to very low sedimentation rates in the region. We calculated rates of 0.003 cm yr^{-1} to 0.006 cm yr^{-1} based on the thickness of the sedimentary layer in between the two turbidites. These rates are similar to those obtained from the Baie de Port-au-Prince for the Holocene at 120 m water depth (Rios et al., 2012). It is also possible that a strike-slip-thrust combination earthquake is required to dislodge sediments, whereas simple strike-slip motion on faults would not have the same effect. Activation of thrust faults that oversteepen the slope on the basin's margins could trigger turbidity currents, resulting in THUs in the Canal du Sud, such as those documented for the 2010 earthquake. This scenario is compatible with the aftershock data, with the coseismic uplift of the adjacent coast (e.g., Hayes et al., 2010), and with geophysical evidence of mass wasting associated with fold growth (Figure 2). Correlation of the two most recent turbidites in the Canal du Sud (McHugh et al., 2011b) with the last two uplift events at Tapion Ridge (Taylor et al., 2011) further supports this scenario. This steep ridge is located at the center of the thrust aftershocks and borders the basin floor 30 km to the southeast (Figures 1C and photo on opening page of this article). Using

Table 1. Excess (xs) ^{234}Th measured in the multicore and gravity core tops*

Core ID	Upper cm	xs^{234}Th (dpm g^{-1})**	1 σ (dpm g^{-1})
MC2-1	0–1	0.70	1.01
MC3-1	0–1	2.36	0.85
MC4-1	0-1	25.63	1.68
MC4-1	1–2	16.20	1.25
MC4-3	0–1	19.94	1.24
MC4-3	1–2	7.83	0.97
MC4-3	2–3	1.88	2.11
MC4-3	3–4	2.88	1.94
MC4-3	5–6	−0.10	0.33
MC4-3	9–10	−0.50	0.42
GC01	0–1	3.30	1.28
GC02	0–1	1.16	1.36
GC03	0–1	4.47	1.43
GC04	0–1	2.03	1.58
GC05	0–1	0.61	1.67
GC06	0–1	−0.23	1.61
GC07	0–1	2.10	1.60
GC08	0–1	1.13	1.49
GC09	0–1	0.98	1.69
GC10	0–1	5.02	1.73
GC11	0–1	2.39	1.65
GC12	0–1	3.90	1.81

*Radionuclide measurements for ^{234}Th were previously published as an appendix in McHugh et al. (2011a), but they were not fully discussed in that *Geology* article.
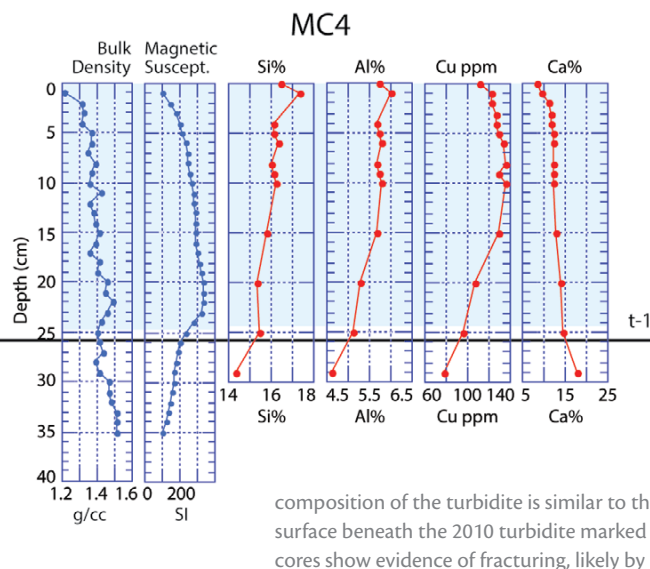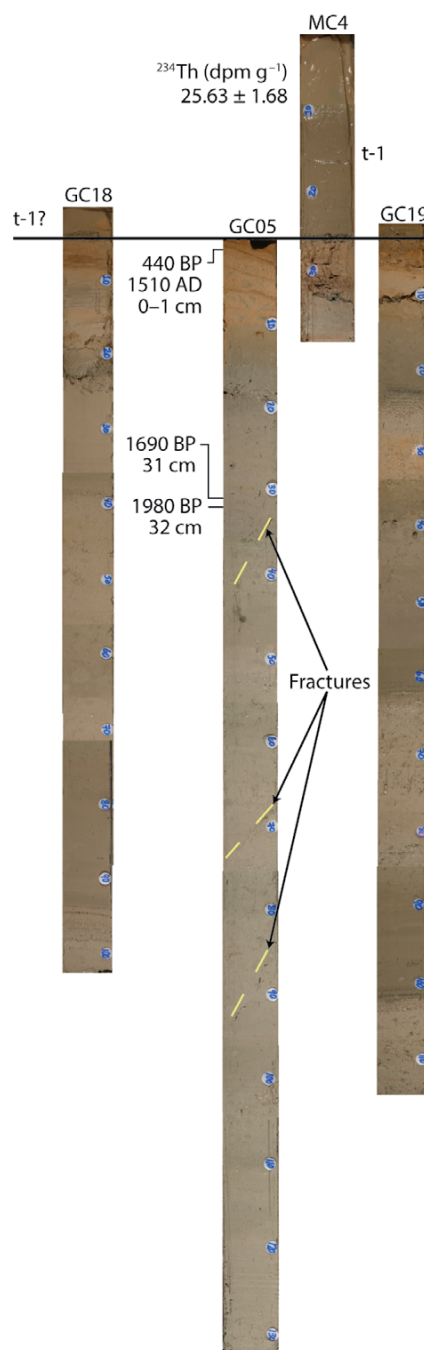** Decays per minute per gram of sediment.

Figure 4. Photos of cores recovered from a fault basin at 1,500 m water depth (Figure 1C). The 2010 turbidite, identified in multicore MC4 from xs^{234}Th, is 25 cm thick and composed of thin basal sand and thick homogeneous mud above. The 2010 turbidite (shaded light blue) is noted in the bulk density and magnetic susceptibility signals by an increase in sand at the base. The elemental composition of the turbidite is similar to that of other 2010 turbidites. The surface beneath the 2010 turbidite marked as t-1 was dated at 1510 CE. The cores show evidence of fracturing, likely by the 2010 earthquake.

coral reef studies, Taylor et al. (2011) documented a 2,100-year recurrence interval for Tapion Ridge uplift events, and McHugh et al. (2011b) documented a ~ 2,000 year interval between THUs in Canal du Sud. Infrequent thrust (uplift) events combined with low sediment supply suggest that earthquakes caused by relative vertical motion on fault blocks facilitate turbidite generation in Canal du Sud. Apparently, the 1751 and 1770 earthquakes in this region did not trigger uplift at the Tapion Ridge or turbidites in Canal du Sud and instead may have been a result of strike-slip motion on faults.

THE NORTH ANATOLIAN FAULT BENEATH THE MARMARA SEA: A BASIN WITH HIGH SEDIMENT SUPPLY AND A LONG RECORD OF HISTORICAL EARTHQUAKES

A large number of paleoseismological studies have focused on the submerged continental transform boundary of the North Anatolian fault (NAF) beneath Turkey's Marmara Sea (Figure 6; e.g., McHugh et al., 2006, 2014; Çağatay et al., 2012). The North Anatolian fault extends for 1,600 km across Turkey and accommodates right lateral motion between Eurasia and the Anatolian Plate at a GPS rate of 23–25 mm yr^{-1} (e.g., Reilinger et al., 2010). The Marmara Sea is an extensional basin related to the northern branch of the North Anatolian fault (Armijo et al., 1999). It is an ideal setting for submarine paleoseismology studies because it contains several small fault-controlled basins that have recorded sedimentation events related to seismic activity along the NAF (Figure 6). These sedimentation events can be calibrated to the historical record of earthquakes that in this region dates back 2,000 years. Sedimentation rates in the Marmara Sea basins are fairly high at 0.16–0.22 cm yr^{-1} (Drab et al., 2012; McHugh et al., 2014).

In the Marmara Sea, THUs were identified and linked to historical earthquakes (McHugh et al., 2006; Sari and Çağatay, 2006; Beck et al., 2007; Çağatay et al., 2012; Drab et al., 2012; Eris et al., 2012). Lithologically, the THU consists of a sharp basal contact above which multiple fining-upward beds of sand to coarse silt are present. This relatively thin and finely stratified basal deposit leads upward into a ~ 50–100 cm thick homogeneous mud unit that is (e.g., McHugh et al., 2006; Çağatay et al., 2012). This internal stratigraphy suggests secondary earthquake-related processes created it, such as multiple slope failures, turbidites that interfere

with each other in the deepest part of the semi-enclosed basins, and/or long wave-length, seiche-like currents (McHugh et al., 2006, 2011a, 2014). Seiche-like currents have also been proposed to explain the stratigraphic relationship between turbidites in Alpine lakes and earthquakes (e.g. Chapron et al., 1999). Through radioisotope dating, THUs in the Marmara Sea have been correlated almost one to one with the historical earthquake record (e.g., Çağatay et al., 2012). The results from the Marmara Sea contrast strikingly with observations in Haiti where significant gaps in the sedimentary earthquake record clearly exist.

CHARACTERIZATION OF PROCESSES AND SEDIMENTARY UNITS TRIGGERED BY EARTHQUAKES

In less than a decade, submarine paleoseismology at transform boundaries has matured from experiment to practice, with the following questions addressed.

Can sedimentation events be recognized in the stratigraphic record, and can they be linked to earthquakes?

In both the Marmara Sea and Canal du Sud, sedimentary units were identified and clearly linked to historical earthquakes. In many cases, the composition of the sand and mud within these deposits has distinct geochemical signatures that allow linking them to a source region, such as a specific river delta. In the case of Haiti, xs^{234}Th allowed us to track the turbidites' paths. The 2010 earthquake caused basin sediment to be suspended in the water column, where the sediment adsorbed additional ^{234}Th. Surprisingly, xs^{234}Th concentrations were lowest in the Canal du Sud basin depocenter. An explanation is that ^{234}Th concentrations in re-suspended basin sediments were diluted by reworked sediment entrained from the margins of the deep basin by the turbidity current and by other mass wasting triggered by the earthquake. These findings reveal that basin sediments are not only derived from shallow water but they are also composed of deep basin sediments re-suspended by earthquakes in Haiti and likely other tectonic basins. These sediments contribute substantially to the regional sedimentation record. In Canal du Sud, Haiti, two months after the 2010
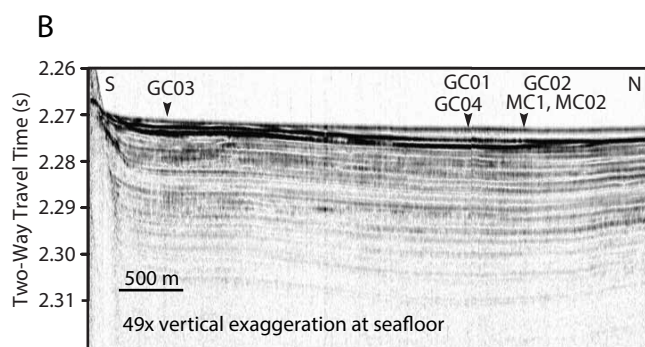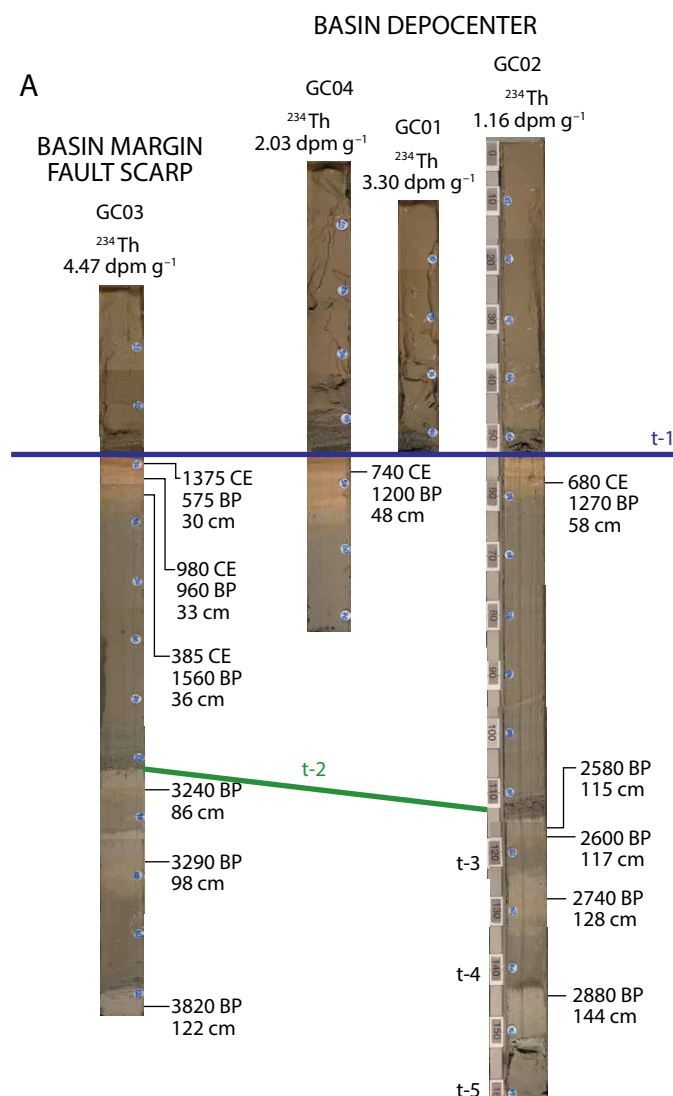

Figure 5. (A) Photos of cores recovered across the Canal du Sud depocenter and along the margins of the basin (GC03). The 2010 turbidite identified from its xs^{234}Th content is characterized by basal sand and ~ 50 cm of homogeneous mud. An anomaly in the beam attenuation of light measured with the CTD transmissometer detected a sediment plume for 1,100 m above the seafloor, showing that mud was still settling two months after the earthquake. The surface t-1 marks the base of the 2010 turbidite and was dated at ~ 1,000 BP. The penultimate turbidite is identical to the 2010 event and its base (marked as t-2) was dated at ~ 2,500 BP. The ages of GC03 are older due to erosion along the margins of the basin. (B) The CHIRP subbottom profile reveals the 2010 turbidite as a semi-transparent layer that covers over 50 km^2 in Canal du Sud.

earthquake, a high concentration of suspended sediment was measured in the water column from 600 m water depth to the seafloor at 1,730 m (McHugh et al., 2011a). Similar sediment-laden waters were linked to earthquakes in the Cariaco Basin (Thunell et al., 1999), offshore Japan after the Tokachi-Oki earthquake (Mikada et al., 2006), above the trench slope near the 2004 epicenter offshore Sumatra (Seeber et al., 2007), and offshore Sendai Bay in association

Table 2. Core ID, radiocarbon age from foraminifers, age error. Years CE and BP

Core ID	¹⁴C Age	Age Error		Calibrated Ages CE/BCE				Calibrated Ages BP		
				Lower Range	Upper Range	Median Probability		Lower Range	Upper Range	Median Probability
GC02-58	1680	28	1 σ	656	709	682	1 σ	1241	1294	1268
			2 σ	621	750	682	2 σ	1200	1329	1268
GC02-115	2790	36	1 σ	−719	−573	−634	1 σ	2522	2668	2583
			2 σ	−752	−497	−634	2 σ	2446	2701	2583
GC02-117	2800	28	1 σ	−726	−601	−653	1 σ	2550	2675	2602
			2 σ	−750	−530	−653	2 σ	2479	2699	2602
GC02-128	2930	28	1 σ	−808	−762	−788	1 σ	2711	2757	2737
			2 σ	−851	−737	−788	2 σ	2686	2800	2737
GC02-144	3080	36	1 σ	−991	−883	−935	1 σ	2832	2940	2884
			2 σ	−1042	−825	−935	2 σ	2774	2991	2884
GC03-30	955	36	1 σ	1338	1411	1374	1 σ	539	612	576
			2 σ	1312	1436	1374	2 σ	514	638	576
GC03-33	1390	31	1 σ	951	1029	984	1 σ	921	999	966
			2 σ	902	1048	984	2 σ	902	1048	966
GC03-36	1970	36	1 σ	341	434	386	1 σ	1516	1609	1564
			2 σ	267	481	386	2 σ	1469	1683	1564
GC03-86	3340	40	1 σ	−1355	−1232	−1288	1 σ	3181	3304	3237
			2 σ	−1400	−1169	−1288	2 σ	3118	3349	3237
GC03-98	3390	40	1 σ	−1398	−1290	−1342	1 σ	3239	3347	3291
			2 σ	−1442	−1225	−1342	2 σ	3174	3391	3291
GC03-122	3830	31	1 σ	−1931	−1819	−1875	1 σ	3768	3880	3824
			2 σ	−1974	−1754	−1875	2 σ	3703	3923	3824
GC04-48	1610	36	1 σ	700	777	741	1 σ	1173	1250	1209
			2 σ	699	833	741	2 σ	1117	1281	1209
GC05-1	760	31	1 σ	1472	1540	1512	1 σ	410	478	438
			2 σ	1456	1616	1512	2 σ	334	494	438
GC05-31	2080	36	1 σ	207	325	258	1 σ	1625	1743	1692
			2 σ	146	364	258	2 σ	1586	1804	1692
GC05-32	2330	31	1 σ	−84	20	−34	1 σ	1930	2033	1983
			2 σ	−141	62	−34	2 σ	1888	2090	1983

Calibrated BCE ranges are noted as negative numbers.
Ages were calibrated using Calib 7.0 from Stuvier and Reimer (2005) with Δr = 31, average uncertainty = 19.
Calibrations show lower range, upper range for 1 σ and 2 σ, and median probability ages.

with the 2011 Tōhoku-Oki earthquake (Ikehara et al., 2013). These plumes of diluted sediment are thought to contribute to the homogenite part of the THU, which appears to be characteristic of confined basins.

How do rates of seismicity and sedimentation affect the correlation between them?

In the Marmara Sea, both sedimentation and earthquake rates are high, and the correlation between the sedimentary record and historical earthquakes is very good over 2,000 years (Sari and Çağatay, 2006; McHugh et al., 2006, 2014; Çağatay et al., 2012; Drab et al., 2012). The sedimentation rate keeps up with the seismicity rate such that most

earthquakes with magnitude > 6.8 trigger THUs, and THUs occur only with earthquakes. Sediment accumulation on steep slopes leads to oversteepening and high pore pressures that in the Marmara Sea never reach criticality for spontaneous failure. Shaking caused by frequent earthquakes (every few centuries) in the region lead to slope failure before criticality is reached. In contrast, relatively low sedimentation and slip rates characterize basins around Haiti. Seismicity rates of the EPGF transform are also lower than those of the NAF. In such low sedimentation regions, only those earthquakes that oversteepen the seafloor and generate greater vertical acceleration are most effective in destabilizing the sediment,

resulting in THUs. This effectiveness depends on earthquake size, but also on other characteristics, such as the direction of shaking relative to the slope and on the permanent deformation of the seafloor associated with the earthquakes. In the case of Haiti, the last two THUs were both results of relatively rare thrust earthquakes, but many intervening strike-slip earthquakes of similar magnitude did not trigger slope failure recognizable in the sedimentary record. An important lesson learned from the EPGF plate boundary is that in low-sedimentation, low-slip-rate transform boundaries, a much longer portion of the fault needs to be investigated in order to recover a more complete earthquake recurrence interval history.
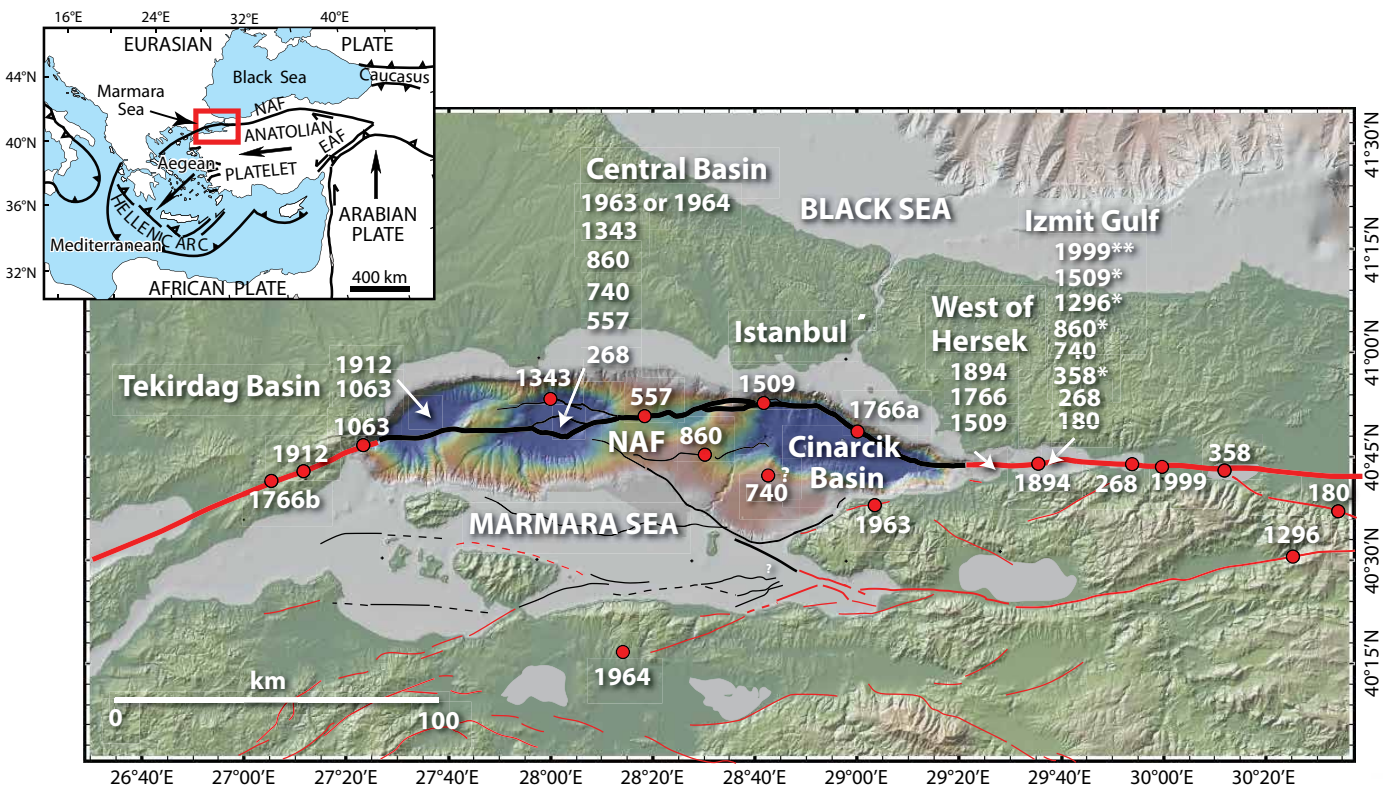
Figure 6. Tectonic setting for the North Anatolian fault (NAF) transform boundary that accommodates right-lateral motion between the Anatolian and Eurasian Plates (inset). The red box shows the location of Marmara Sea relative to the plate boundary (modified from McHugh et al., 2014). The Marmara Sea is crossed by the North Anatolian fault and is composed of three main basins (from west to east, Tekirdag, Central, and Cinarcik) as well as the Izmit Gulf. The basins are ~ 1,200 m deep and are semi-enclosed. In the Marmara Sea, there is very good correlation between historical earthquakes (red dots) and turbidite-homogenite units in the adjacent basin. Arrows mark the locations where turbidite-homogenite units (THUs) were recovered. The ages of the historical earthquakes that correlate with the THUs are shown in white.

Do segment-rupturing earthquakes generate submarine sediment slope failures and sedimentation events, and can this record be documented?

One of the main objectives of the submarine paleoseismology field is to link a sedimentation event to the rupture on a specific fault segment. Fault segments tend to be longer along convergent plate boundaries, and in those regions, paleoseismology is closer to reaching that goal (e.g., Goldfinger et al., 2007). But even at transform boundaries, evidence linking sedimentation events and specific fault segments is increasing. For example, in the Marmara Sea, very good correlation was established between THUs in a basin and in proximal inferred historical ruptures, to the point that multisegment ruptures could be identified (McHugh et al., 2014). In Canal du Sud, a correlation was also found between a fault segment and sedimentation events in the adjacent basin. This correlation is limited to approximately every 2,000 years, and other plate boundary segments need to be investigated so that earthquake ruptures can be completely represented. These new findings have the potential to contribute substantially to future progress in the field of submarine paleoseismology.

CONCLUDING REMARKS

Submarine paleoseismology along submarine continental transform boundaries has made much progress in the past 10 years. This research has provided information about how earthquakes influence sedimentation and about the long-term seismogenic behavior of fault systems, which can aid in seismic hazard evaluation. Submarine imaging techniques have captured in unprecedented detail faults and fault-related structures such as

anticlines and basins, and the pathways that transport sediment. Dating and sampling techniques have enabled us to track the path of earthquake-generated sedimentation from the nearshore to the depocentral regions of basins in Canal du Sud, Haiti. The long historical earthquake records available for Turkey correlate well with sedimentation events for threshold earthquakes of magnitude > 6.8, showing that high sedimentation rates allow documentation of earthquake recurrence intervals. In settings with low sedimentation rates, as in Canal du Sud, only a subset of earthquakes are effective in de-stabilizing sediments sufficiently to trigger sedimentation events. Therefore, longer segments of that plate boundary need to be investigated. Transform boundary faults are segmented, and increasing evidence allows a sedimentation event to be connected to an adjacent fault segment. Submarine paleoseismology has successfully emerged from the initial experimental phase and is poised to bear many fruits. Promising directions include obtaining earthquake records that are long enough to cover the growth of a fault-related structure, such as a transform basin; achieving better resolution of rupture length; and extracting more complete earthquake-triggered sedimentation records in low sediment supply and low slip rate margins by sampling different segments of the plate boundary.

REFERENCES

Ambraseys, N.N. 2002. The seismic activity in the Marmara Sea region over the last 2000 years. *Bulletin of the Seismological Society of America* 92:1–18, http://dx.doi.org/10.1785/0120000843.

Armijo, R., B. Meyer, A. Hubert, and A.A. Barka. 1999. Westward propagation of the north Anatolian fault into the northern Aegean: Timing and kinematics. *Geology* 27:267–270, http://dx.doi.org/10.1130/0091-7613(1999)027<0267:WPOTNA>2.3.CO;2.

Bakum, W.H., C.H. Flores, and U.S. ten Brink. 2012. Significant earthquakes on the Enriquillo fault system, Hispaniola, 1500–2010: Implications for seismic hazard. *Bulletin of the Seismological Society of America* 102:18–30, http://dx.doi.org/10.1785/0120110077.

Barka, A.A. 1999. The 17 August 1999 Izmit earthquake. *Science* 285:1,858–1,859, http://dx.doi.org/10.1126/science.285.5435.1858.

Barnes, P.M., H.C. Bostock, H.L. Neil, L.J. Strachan, and M. Gosling. 2013. A 2300-year paleoearthquake record of the Southern Alpine fault and Fiordland subduction zone, New Zealand, based on stacked turbidites. *Bulletin of the Seismological Society of America* 10:2,434–2,446, http://dx.doi.org/10.1785/0120120314.

Beck, C., B. Mercier de Lépinay, J.L. Schneider, M. Cremer, M.N. Çağatay, E. Wendenbaum, S. Boutareaud, G. Menot, S. Schmidt, O. Weber, and others. 2007. Late Quaternary co-seismic sedimentation in the Sea of Marmara's deep basins. *Sedimentary Geology* 199:65–89, http://dx.doi.org/10.1016/j.sedgeo.2005.12.031.

Brothers, D.S., N.W. Driscoll, G.M. Kent, A.J. Harding, J.M. Babcock, and R.L. Baskin. 2009. Tectonic evolution of the Salton Sea inferred from seismic reflection data. *Nature Geoscience* 2:581–584, http://dx.doi.org/10.1038/ngeo590.

Çağatay, M.N., L. Erel, L.G. Bellucci, A. Polonia, L. Gasperini, K.K. Eris, U. Sancar, D. Biltekin, G. Uçarkus, U.B. Ulgen, and E. Damci. 2012. Sedimentary earthquake records in the Izmit Gulf, Sea of Marmara, Turkey. *Sedimentary Geology* 282:347–359, http://dx.doi.org/10.1016/j.sedgeo.2012.10.001.

Calais, E., A. Freed, G. Mattioli, F. Amelung, S. Jonsson, P. Jansma, S.-H. Hong, T. Dixon, C. Prepetit, and R. Momplaisir. 2010. Transpressional rupture of an unmapped fault during the 2010 Haiti earthquake. *Nature Geoscience* 3:794–799, http://dx.doi.org/10.1038/ngeo992.

Chapron, E., C. Beck, M. Pouchet, and J.F. Deconninck. 1999. 1822 earthquake-triggered homogenite in Lake Le Bouget (NW Alps). *Terra Nova* 11:86–92, http://dx.doi.org/10.1046/j.1365-3121.1999.00230.x.

Cormier, M.-H., L. Seeber, C.M.G. McHugh, A. Polonia, M.N. Çağatay, O. Emre, L. Gasperini, N. Görür, G. Bortoluzzi, E. Bonatti, and others. 2006. North Anatolian fault in the Gulf of Izmit (Turkey): Rapid vertical motion in response to minor bends of a non-vertical continental transform. *Journal of Geophysical Research* 111, B04102, http://dx.doi.org/10.1029/2005JB003633.

DeMets, C., P. Jansma, G. Mattioli, T. Dixon, F. Farina, R. Bilham, E. Calais, and P. Mann. 2000. GPS geodetic constraints on Caribbean-North America plate motion. *Geophysical Research Letters* 27:437–440, http://dx.doi.org/10.1029/1999GL005436.

Dixon, T.H., F. Farina, C. DeMets, P. Jansma, P. Mann, and E. Calais. 1998. Relative motion between the Caribbean and North American plates and related boundary zone deformation from a decade of GPS observations. *Journal of Geophysical Research* 103(B7):15,157–15,182, http://dx.doi.org/10.1029/97JB03575.

Douilly, R., J.S. Haase, W.L. Ellsworth, M.-P. Bouin, E. Calais, S.J. Symithe, J.G. Armbruster, B.M. de Lepinay, A. Deschamps, S.-L. Mildor, and others. 2013. Crustal structure and fault geometry of the 2010 Haiti earthquake from temporary seismometer deployments. *Bulletin of the Seismological Society of America* 103:2,305–2,325, http://dx.doi.org/10.1785/0120120303.

Drab, L., A. Hubert-Ferrari, S. Schmidt, and P. Martinez. 2012. The earthquake record in the western part of the Sea of Marmara, Turkey. *Natural Hazards and Earth System Sciences* 12:1,235–1,254.

Eris, K.K., N. Çağatay, C. Beck, B. Mercier de Lépinay, and C. Campos. 2012. Late-Pleistocene to Holocene sedimentary fills of the Cinarcik Basin of the Sea of Marmara. *Sedimentary Geology* 281:151–165, http://dx.doi.org/10.1016/j.sedgeo.2012.09.001.

Escalona, A., P. Mann, and M. Jaimes. 2011. Miocene to recent Cariaco basin, offshore Venezuela: Structure, tectonosequences and basin-forming mechanisms. *Marine and Petroleum Geology* 28:177–199, http://dx.doi.org/10.1016/j.marpetgeo.2009.04.001.

Goldfinger, C., A.E. Morey, C.H. Nelson, J. Gutiérrez-Pastor, J.E. Johnson, E. Karabanov, J. Chaytor, and A. Ericsson. 2007. Rupture lengths and temporal history of significant earthquakes on the offshore and north coast segments of the northern San Andreas fault based on turbidite stratigraphy. *Earth and Planetary Science Letters* 254:9–27, http://dx.doi.org/10.1016/j.epsl.2006.11.017.

Goldfinger, C., C.H. Nelson, and J.E. Johnson. 2003. Holocene earthquake records from the Cascadia subduction zone and northern San Andreas fault based on precise dating of offshore turbidites. *Annual Review of Earth and Planetary Science* 31:555–577, http://dx.doi.org/10.1146/annurev.earth.31.100901.141246.

Goldfinger, C., C.H. Nelson, A.E. Morey, J.R. Johnson, J. Patton, E. Karabanov, J. Gutiérrez-Pastor, A.T. Erikson, E. Gracia, G. Dunhill, and others. 2012. Turbidite event history: Methods and implications for Holocene paleoseismicity of the Cascadia subduction zone. *US Geological Survey Professional Paper* 1661-F:1–170. Available at http://pubs.usgs.gov/pp/pp1661f.

Gracia, E., A. Vizcaino, C. Escutia, A. Asioi, A. Rodes, R. Pallas, J. Garcia-Orellana, S. Lebreiro, and C. Goldfinger. 2010. Holocene earthquake record offshore Portugal (SW Iberia): Testing turbidite paleoseismology in a slow-convergence margin. *Quaternary Science Reviews* 29:1,156–1,172.

Gutiérrez-Pastor, J., C.H. Nelson, C. Goldfinger, and C. Escutia. 2013. Sedimentology of seismo-turbidites off the Cascadia and Northern California active tectonic continental margins, Northwest Pacific Ocean. *Marine Geology* 336:99–119, http://dx.doi.org/10.1016/j.margeo.2012.11.010.

Hashimoto, M., Y. Fukushima, and Y. Fukahata. 2011. Fan-delta uplift and mountain subsidence during the Haiti 2010 earthquake. *Nature Geoscience* 4:255–259, http://dx.doi.org/10.1038/ngeo1115.

Hayes, G.P., R.W. Briggs, A. Sladen, E.J. Fielding, C.S. Prentice, K.W. Hudnut, P. Mann, F.W. Taylor, A.J. Crone, R.D. Gold, and others. 2010. Complex rupture during the 12 January 2010 Haiti earthquake. *Nature Geoscience* 3:800–805, http://dx.doi.org/10.1038/ngeo977.

Hornbach, M.J., N. Braudy, R.W. Briggs, M.-H. Cormier, M.B. Davis, J.B. Diebold, N. Dieudonne, R. Douilly, C. Frohlich, S.P.S. Gulick, and others. 2010. High tsunami frequency as a result of combined strike-slip faulting and coastal landslides. *Nature Geoscience* 3:783–788, http://dx.doi.org/10.1038/ngeo975.

Hough, S.E., J.R. Altidor, D. Anglade, D. Given, M.G. Guillard, Z. Maharrey, M. Meremonte, B.S.-L. Mirador, C. Prépetit, and A. Yong. 2010. Localized damage caused by topographic amplification during the 2010 M 7.0 Haiti earthquake. *Nature Geoscience* 3:778–782, http://dx.doi.org/10.1038/ngeo988.

Ikehara, K., K. Usami, and T. Irino. 2013. Sediment resuspension, transportation and redeposition by tsunami: Example from the 2011 Tohoku-Oki tsunami on Sendai and Sanriku shelves. Abstract 1800306, Fall Meeting of the American Geophysical Union, San Francisco, CA.

Koehler, R.D., P. Mann, C.S. Prentice, L. Brown, B. Benford, and M. Wiggins-Grandison. 2012. Enriquillo-Plantain Garden fault zone in Jamaica: Paleoseismology and seismic hazard. *Bulletin of the Seismological Society of America* 103:971–983, http://dx.doi.org/10.1785/0120120215.

Manaker, D.M., E. Calais, A.M. Freed, S.T. Ali, P. Przybylski, G.S. Mattioli, P. Jansma, C. Prépetit, and J.B. de Chabalier. 2008. Interseismic plate coupling in the northeast Caribbean. *Geophysical Journal International* 174:889–903, http://dx.doi.org/10.1111/j.1365-246X.2008.03819.x.

Mann, P., F.W. Taylor, R.L. Edwards, and T.L. Ku. 1995. Actively evolving microplate formation by oblique collision and sideways motion along strike-slip faults: An example from the northeastern Caribbean plate margin. *Tectonophysics* 246:1–69, http://dx.doi.org/10.1016/0040-1951(94)00268-E.

McHugh, C.M.G., N. Braudy, M.N. Çağatay, C. Sorlien, M.-H. Cormier, L. Seeber, and P. Henry. 2014. Seafloor fault ruptures along the North Anatolia fault in the Marmara Sea, Turkey: Link with the adjacent basin turbidite record. *Marine Geology* 353:65–83, http://dx.doi.org/10.1016/j.margeo.2014.03.005.

McHugh, C.M., L. Seeber, N. Braudy, M.-H. Cormier, M.B. Davis, N. Dieudonne, J. Deming, J.B. Diebold, R. Douilly, S.P.S. Gulick, and others. 2011a. Offshore sedimentary effects of the 12 January Haiti earthquake. *Geology* 39:723–726, http://dx.doi.org/10.1130/G31815.1.

McHugh, C.M.G., L. Seeber, M.-H. Cormier, J. Dutton, M.N. Çağatay, A. Polonia, W.B.F. Ryan, and N. Görür. 2006. Submarine earthquake geology along the North Anatolia Fault in the Marmara Sea, Turkey: A model for transform basin sedimentation. *Earth and Planetary Science Letters* 248:661–684, http://dx.doi.org/10.1016/j.epsl.2006.05.038.

McHugh, C.M., L. Seeber, M.-H. Cormier, M.H. Hornbach, R. Momplaisir, F. Waldhaourser, C. Sorlien, M. Steckler, and S. Gulick. 2011b. A Seismo-tectonic signal from offshore sedimentation: The 2010 Haiti earthquake and prior events. Abstract T33G-2492, Fall Meeting of the American Geophysical Union, San Francisco CA.

Mercier de Lépinay, B., A. Deschamps, F. Klingelhoefer, Y. Mazabraud, B. Delouis, V. Clouard, Y. Hello, J. Crozon, B. Marcaillou, D. Graindorge, and others. 2011. The 2010 Haiti earthquake: A complex fault pattern constrained by seismologic and tectonic observations. *Geophysical Research Letters* 38, L22305, http://dx.doi.org/10.1029/2011GL049799.

Mikada, H., K. Mitsuzawa, H. Matsumoto, T. Watanabe, S. Morita, R. Otsuka, H. Sugioka, T. Baba, E. Araki, and K. Suyehiro. 2006. New discoveries in dynamics of a M8 earthquake-phenomena and their implications from the 2003 Tokachi-Oki earthquake using a long term monitoring cabled observatory. *Tectonophysics* 426:95–105, http://dx.doi.org/10.1016/j.tecto.2006.02.021.

Noda, A., T. TuZino, Y. Kanai, R. Furukawa, and J. Uchida. 2008. Paleoseismicity along the southern Kuril Trench deduced from submarine-fan turbidites. *Marine Geology* 204:73–90, http://dx.doi.org/10.1016/j.margeo.2008.05.015.

Parsons, T., S. Toda, R.S. Stein, A.A. Barka, and J.H. Dieterich. 2000. Heightened odds of large earthquakes near Istanbul: An interaction-based probability calculation. *Science* 288:661–665, http://dx.doi.org/10.1126/science.288.5466.661.

Patton, J.R., C. Goldfinger, A. Morey, C. Romsos, B. Black, Y.S. Djadjadihardja, and U. Udrekh. 2013. Seismoturbidite record as preserved at core sites at the Cascadia and Sumatra-Andaman subduction zones. *Natural Hazards and Earth System Sciences* 13:833–867, http://dx.doi.org/10.5194/nhess-13-833-2013.

Plesch, A., J.H., Shaw, C. Benson, W.A. Bryant, S. Carena, M. Cooke, J. Dolan, G. Fuis, E. Gath, L. Grant, and others. 2007. Community Fault Model (CFM) for Southern California. *Bulletin of the Seismological Society of America* 97:1,793–1,802, http://dx.doi.org/10.1785/0120050211.

Prentice, C.S., P. Mann, A.J. Crone, R.D. Gold, K.W. Hudnut, R.W. Briggs, R.D. Koehler, and P. Jean. 2010. Seismic hazard of the Enriquillo–Plantain Garden fault in Haiti inferred from paleoseismology. *Nature Geoscience* 3:789–793, http://dx.doi.org/10.1038/ngeo991.

Polonia, A., G. Panieri, L. Gasperini, G. Gasparotto, L.G. Bellucci, and L. Torelli. 2012. Turbidite paleoseismology in the Calabrian Arc Subduction Complex (Ionian Sea). *Geochemistry, Geophysics, Geosystems* 14:1,525–2,027, http://dx.doi.org/10.1029/2012GC004402.

Pouderoux, H., G. Lamarche, and J.-N. Proust. 2012. Building an 18,000-year-long paleo-earthquake record from detailed deep-sea turbidite characterisation in Poverty Bay, New Zealand. *Natural Hazards Earth System Science* 12:2,077–2,101, http://dx.doi.org/10.5194/nhess-12-2077-2012.

Reilinger, R.E., M.N. Toksöz, S.C. McClusky, and A.A. Barka. 2000. 1999 Izmit, Turkey earthquake was no surprise. *GSA Today* 10:1–6.

Reilinger, R., S. McClusky, D. Paradissis, S. Ergintav, and P. Vernant. 2010. Geodetic constraints on the tectonic evolution of the Aegean region and strain accumulation along the Hellenic subduction zone. *Tectonophysics* 488:22-30, http://dx.doi.org/10.1016/j.tecto.2009.05.027.

Rios, J.K., C.M. McHugh, L. Seeber, S. Blair, and C.C. Sorlien. 2012. Latest Pleistocene to Holocene evolution of the Baie de Port au Prince, Haiti. Abstract T41A-2572, American Geophysical Union Fall Meeting, San Francisco CA.

Sari, E., and M.N. Çağatay. 2006. Turbidites and their association with past earthquakes in the deep Cinarcik Basin of the Marmara Sea. *Geo-Marine Letters* 26:69–76, http://dx.doi.org/10.1007/s00367-006-0017-3.

Schubert, C. 1982. Neotectonics of Boconó fault, western Venezuela. *Tectonophysics* 85:205-220.

Seeber, L., M.-H. Cormier, C. McHugh, Ö. Emre, A. Polonia, and C. Sorlien 2006. Rapid subsidence and sedimentation from oblique slip near a bend on the North Anatolian transform fault in the Marmara Sea, Turkey. *Geology* 34:933–936, http://dx.doi.org/10.1130/G22520A.1.

Seeber, L., C. Mueller, T. Fujiwara, K. Arai, W. Sohn, Y. S. Djajadihardja, and M.-H. Cormier. 2007. Accretion, mass wasting, and partitioned strain over the 26 Dec 2004 M_W 9.2 rupture offshore Aceh, northern Sumatra. *Earth Planetary Science Letters* 263:16–31, http://dx.doi.org/10.1016/j.epsl.2007.07.057.

St-Onge, G., E. Chapron, S. Mulsow, M. Salas, M. Viel, M. Debret, A. Foucher, T. Mulder, T. Winiarski, M. Desmet, and others. 2012. Comparison of earthquake-triggered turbidites from the Saguenay (eastern Canada) and Reloncavi (Chilean margin) fjords: Implications for paleoseismicity and sedimentology. *Sedimentary Geology* 243–244:9–107, http://dx.doi.org/10.1016/j.sedgeo.2011.11.003.

Strasser, M., M. Kölling, C. dos Santos Ferreira, H.G. Fink, T. Fujiwara, S. Henkel, K. Ikehara, T. Kanamatsu, K. Kawamura, S. Kodaira, and others. 2013. A slump in the trench: Tracking the impact of the 2011 Tohoku-Oki earthquake. *Geology* 41:935–938, http://dx.doi.org/10.1130/G34477.1.

Taylor, F.W., P. Mann, R.W. Briggs, C.S. Prentice, P. Jean, C.-C. Shen, H.W. Chiang, and X.-Y. Jiang 2011. Late Holocene paleo-uplift events at the Tapion restraining bend in Haiti: Implications for earthquake recurrence in the vicinity of the 2010 rupture zone. Abstract T33G-2491, Fall Meeting of the American Geophysical Union, San Francisco CA.

Thunell, R., E. Tappa, R. Varela, M. Llano, Y. Astor, F. Muller-Karger, and R. Bohrer. 1999. Increased marine sediment suspension and fluxes following an earthquake. *Nature* 398:233–236, http://dx.doi.org/10.1038/18430.

Vila, J.-M., J. Butterlin, T. Calmus, B. Mercier de Lépinay, and B. Van den Berghe. 1985. Carte geologique d'Haiti au 1/1,000,000 avec notice explicative detaille. In *Atlas d'Haiti*. C. Girault, ed., Publication of CEGET-CNRS, Bordeaux, France.